Supporting Information For:

Catalytic Deoxyribozyme-modified Nanoparticles for RNAi-Independent Gene Regulation

Kevin Yehl[†], Jayashree P. Joshi[‡,Γ], Brandon L. Greene[†], R. Brian Dyer[†], Rita Nahta[‡,Γ,#] and Khalid Salaita[†,‡,*]

[†]Department of Chemistry, [‡]Winship Cancer Institute, [Γ]Department of Pharmacology, [#]Department of Hematology and Medical Oncology, Emory University, Atlanta, GA 30322, United States

This file includes:
SI Materials
SI Table 1
SI Figures 1-10

Materials

All chemicals were purchased from Sigma-Aldrich unless otherwise noted. Stock solutions were made using Nanopure water (Barnstead Nanopure system,18.2 MΩ). The DNA fluorescence assay kit (Quant-iT™ OliGreen® ssDNA kit) was acquired from Life Technologies (formerly Invitrogen, Carlsbad, CA) and was used to quantify DNAzyme density in each batch of DNAzyme gold nanoparticle (DzNP) conjugate that was synthesized. HCC1954 (CRL 2338) cells were obtained from ATCC and media supplies purchased from (Mediatech, Inc., Manassas, VA). All oligonucleotides were custom synthesized by Integrated DNA Technologies (IDT) and are summarized in SI Table 1.

SI Table 1

ID	Sequence (5'-3')
DzT_{10} (Free)	GCACCCAGGCTAGCTACAACGACTCTCTCT$_{10}$
DzT_{10}	GCACCCAGGCTAGCTACAACGACTCTCTCT$_{10}$(CH$_2$)$_3$SH
$Dz_{rev}T_{10}$	HS(CH$_2$)$_6$T$_{10}$GCACCCAGGCTAGCTACAACGACTCTCTC
DzT_{20}	GCACCCAGGCTAGCTACAACGACTCTCTCT$_{20}$(CH$_2$)$_3$SH
$DzT_{10}N_{40}$	GCACCCAGGCTAGCTACAACGACTCTCTCN$_{40}$T$_{10}$(CH$_2$)$_3$SH
$Dz((EG)_6PO_3)_3$	GCACCCAGGCTAGCTACAACGACTCTCTC((EG)$_6$PO$_3$)$_3$(CH$_2$)$_3$SH
T_{10}	T$_{10}$(CH$_2$)$_3$SH
Substrate	6FAM-GAGAGAGrArUGGGTGC-BHQ
Calibration Probe	GAGAGAGAUGGGTGC-6FAM
Dz_{GDF15}	mGmAGTGCAAGGCTAGCTACAACGATCTGAGGGT$_8$mUmU(CH$_2$)$_3$SH
i-Dz_{GDF15}	mGmAGTGCAA**A**GCTAGCTACAACGATCTGAGGGT$_8$mUmU(CH$_2$)$_3$SH
Dz_{NC}	mNmNNNNNNNNGGCTAGCTACAACGANNNNNNNNT$_8$mUmU(CH$_2$)$_3$SH

r=ribonucleotide, 6FAM=6-carboxyfluorescein, BHQ=Black Hole Quencher™, m=2'-O-methyl RNA base, red=catalytic core, **underlined and bold**= inactive point mutation

All DNA and AuNP concentrations were determined by measuring UV absorption using a NanoDrop 2000C. JEOL JEM-1210 transmission electron microscope (TEM) was used to measure the mean AuNP size and polydispersity. A Bio-Tek® Synergy HT temperature controlled plate reader was used to measure fluorescence intensity as a function of time for catalysis time-course studies.

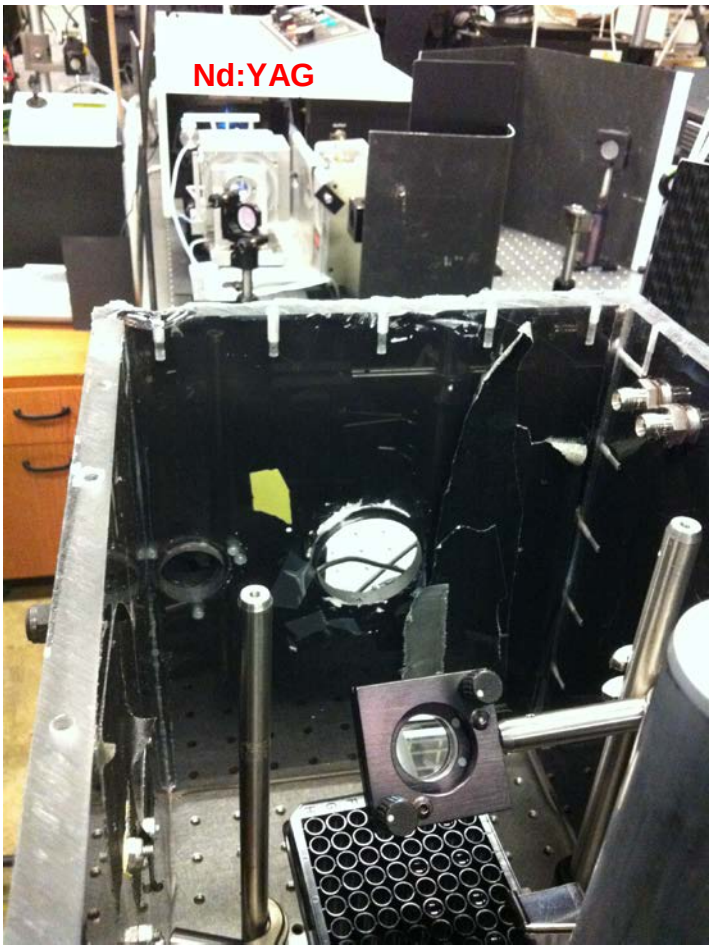

Laser set up for photo-activated DNAzymes.

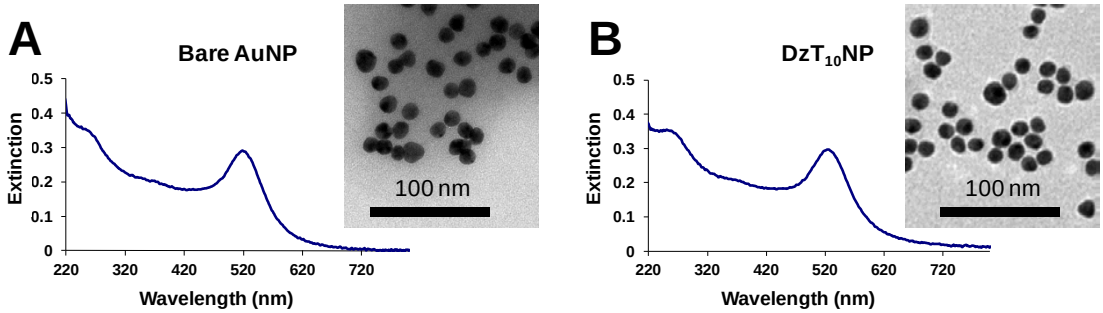

Figure S1. NP characterization. Representative UV-vis spectrum and TEM of citrate stabilized gold nanoparticles (A) and DzT_{10} modified gold nanoparticles (B).

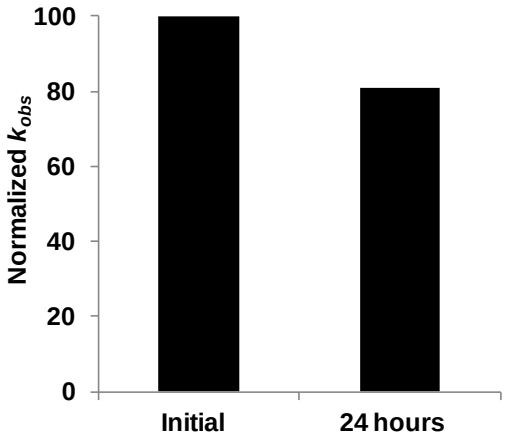

Figure S2. Stability of DzNP. A bar graph showing the initial and final catalytic activity of $Dz((EG_6)PO_3)_3NP$ after incubation at 25 °C for 24 hrs during a catalytic run. At *t* = 24 hrs, the nanoparticles were isolated and used in another reaction with new substrate in reaction buffer (20 mM Tris pH 7.4, 300 mM NaCl, and 10 mM $MgCl_2$) and the initial rate constant of the reaction was reported.

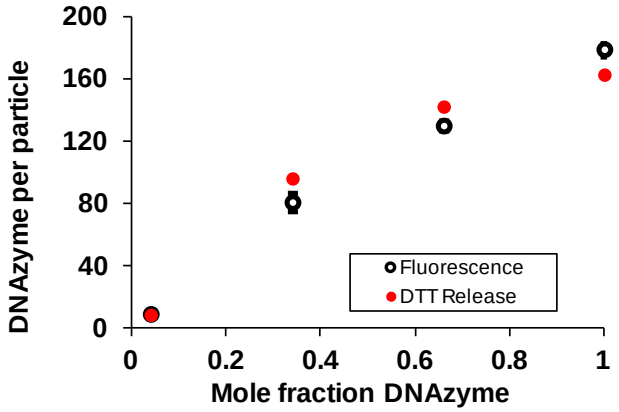

Figure S3. Controlling DNAzyme density on nanoparticle surface. A plot showing the DNAzyme surface density as determined by two independent methods. The first method is based on an oligonucleotide fluorescence quantification kit (open circles). The second approach measures the catalytic activity of DTT-released DNAzyme and the concentration was quantified using a standard calibration curve (red circles). Error bars represents the standard deviation of three measurements.

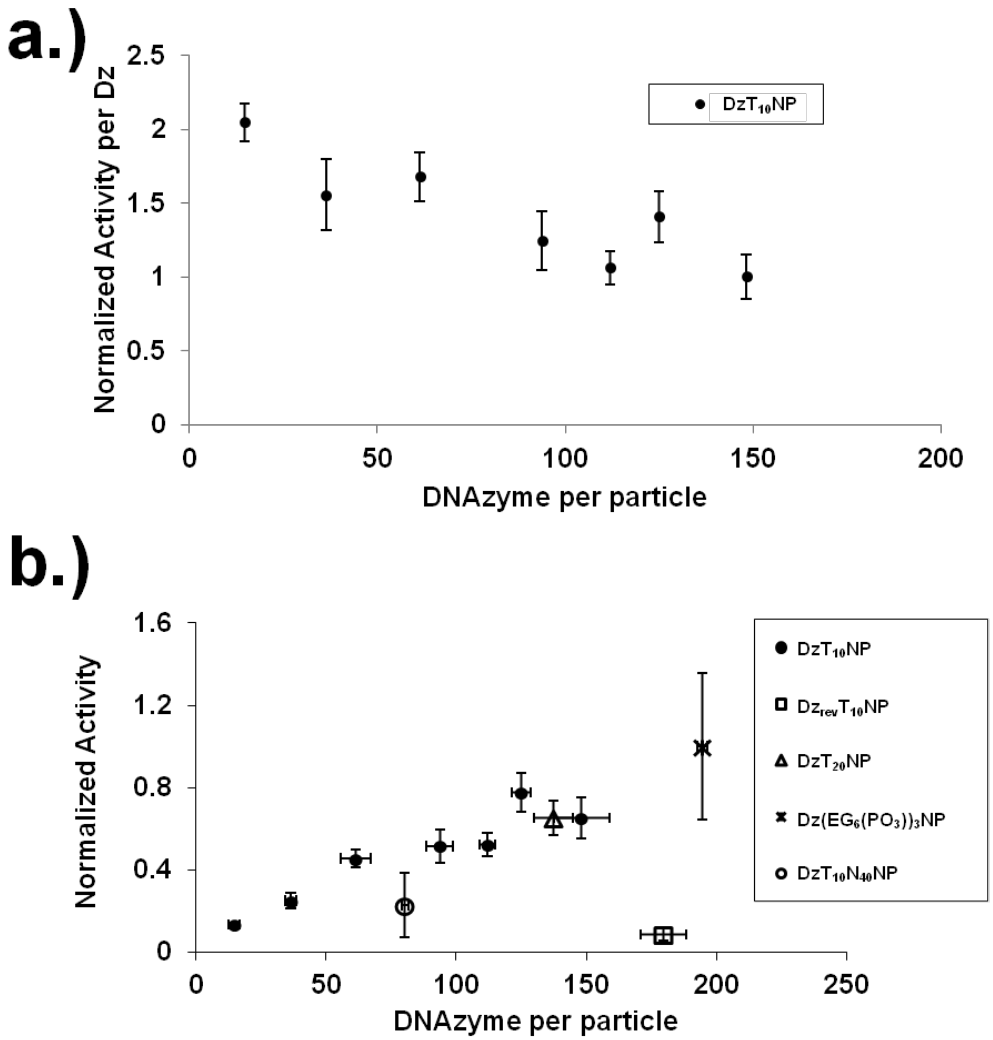

Figure S4. Effects of packing density, orientation, and chemical linker on DzNP catalytic activity. (a) Catalytic activity per DNAzyme of a series of DzT_{10}NPs that vary in DNAzyme surface density. The k_{obs} values were normalized to the activity of Dz from the non-passivated, fully packed particle (4.2×10^{-4} min^{-1}). Error bars are the standard deviation of three measurements. (b) Catalytic activity of DzNPs synthesized using a variety of different linkers ([$MgCl_2$]=10mM). The k_{obs} values were normalized to the activity of the most efficient particle: $Dz((EG_6)PO_3)_3NP$ (99.4×10^{-3} min^{-1}).

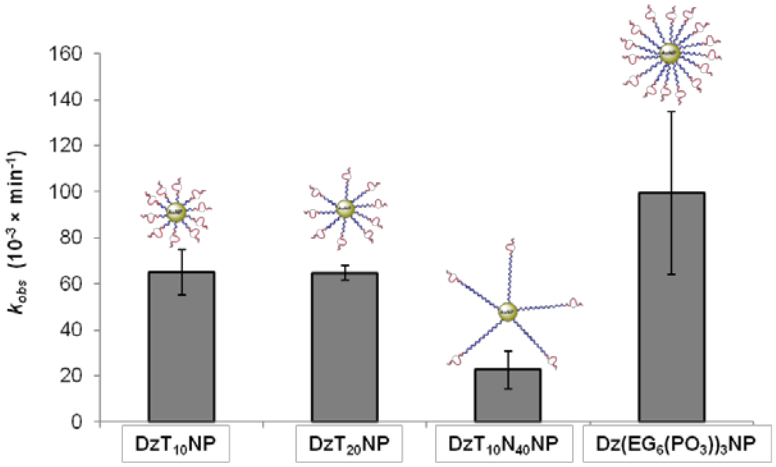

I.D.	#DNA/NP
DzT$_{10}$NP	148±10
DzT$_{20}$NP	137±10
DzT$_{10}$N$_{40}$NP	80±1
Dz(EG$_6$(PO$_3$))$_3$	195±2

Figure S5. Effects of linker on DzNP catalytic activity. A bar graph summarizing the catalytic activity of DzNPs synthesized using a variety of different linkers with schematic representations of the fully packed DzNPs showing DNAzyme (red) density and linker (blue) length. The k_{obs} values were calculated by measuring the linear slope of the initial rate of reaction from the kinetic plot (t<80 min.) divided by particle concentration ([$MgCl_2$]=10mM). Error bars are the standard deviation of three measurements. The table summarizes the corresponding DNA densities.

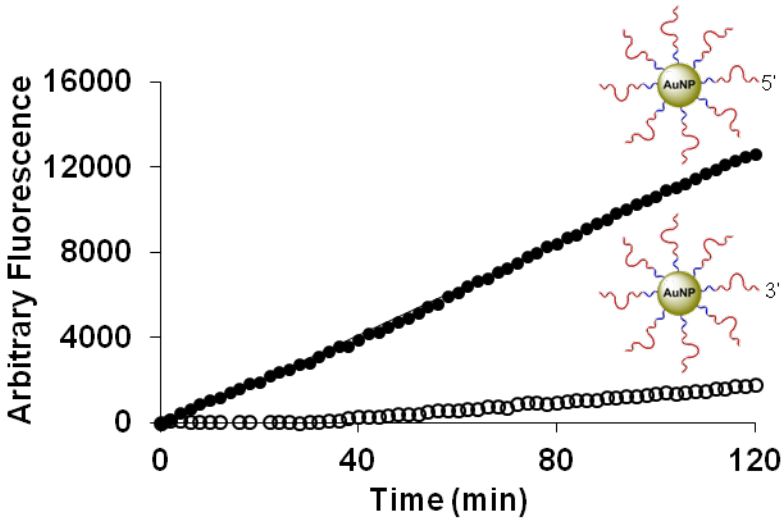

Figure S6. Effect of DNAzyme orientation on catalytic activity of DzNP. A kinetic plot showing the rate of hydrolysis of a quenched substrate for $DzT_{10}NP$ (Dz anchored through the 3' terminus, open circles) and $Dz_{rev}T_{10}NP$ (Dz anchored through the 5' terminus, closed circles). The DNAzyme surface density was similar for both particles.

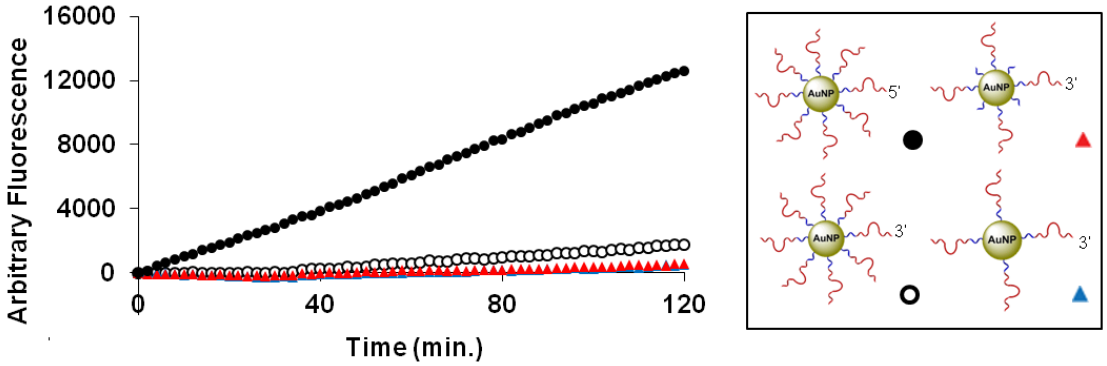

Figure S7. Catalysis of fully packed and 50% packed $Dz_{rev}T_{10}NP$. A kinetic plot showing the rate of hydrolysis of a quenched substrate for fully packed $Dz_{rev}T_{10}$ NP (open circles) and 50% packed (T_{10} passivated: closed red triangles and non-passivated: closed blue triangles) $Dz_{rev}T_{10}NP$. The data indicates that the reduction in steric crowding does not restore $Dz_{rev}T_{10}NP$'s activity to the level of $DzT_{10}NP$ (closed black circles).

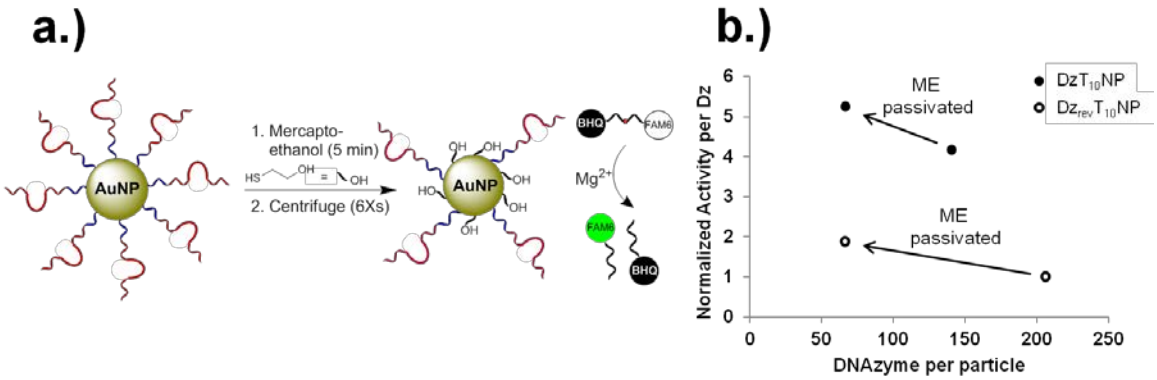

Figure S8. Activity of mercaptoethanol (ME) passivated DzNPs. (a) A schematic showing the use of ME passivation of DzNP to reduce Dz-Au interactions. The catalytic activity of the passivated particles was determined by measuring the rate of fluorescence increase, which represents the rate of substrate hydrolysis and de-quenching. (b) A plot showing the increase in catalytic activity per DNAzyme molecule of $DzT_{10}NP$ and $Dz_{rev}T_{10}NP$ after passivation with mercaptoethanol (ME) normalized to nonpassivated $Dz_{rev}T_{10}NP$ (0.75 nM DzNP, 20 mM CHES pH 8.6, 150 mM NaCl, and 50 mM $MgCl_2$).

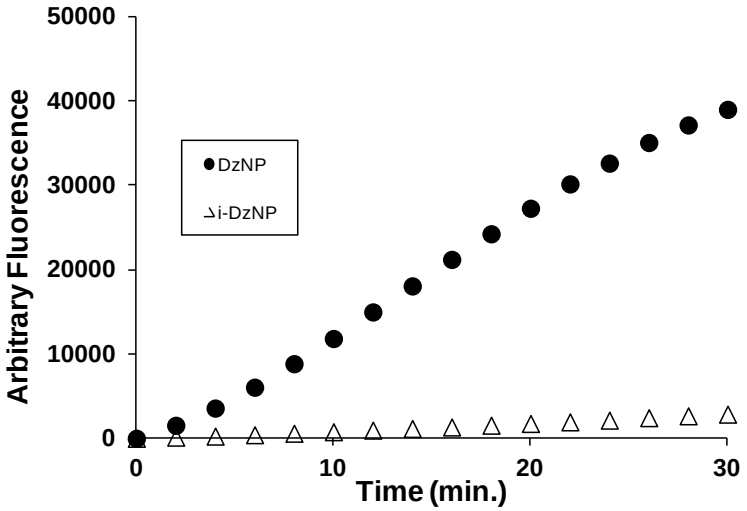

Figure S9. DzNP stability in serum. A kinetic plot showing the rate of hydrolysis of a quenched substrate for active (DzNP) and inactive (i-DzNP) DzNPs. Both particles were treated with cell culture media (DMEM) supplemented with 10% fetal bovine serum (FBS) for 24 hours at a particle concentration of 1.25 nM and a total volume of 500 µL. After 24 hours, the particles were centrifuged down and media was discarded and reaction buffer added, thus bringing the final particle concentration to 4.2 nM and standard reaction conditions (1 µM substrate, 20 mM Tris pH 7.4, 300 mM NaCl, and 10 mM $MgCl_2$). The slight background rate observed for the in-active DzNPs is the result of residual RNase that is typically found in serum.

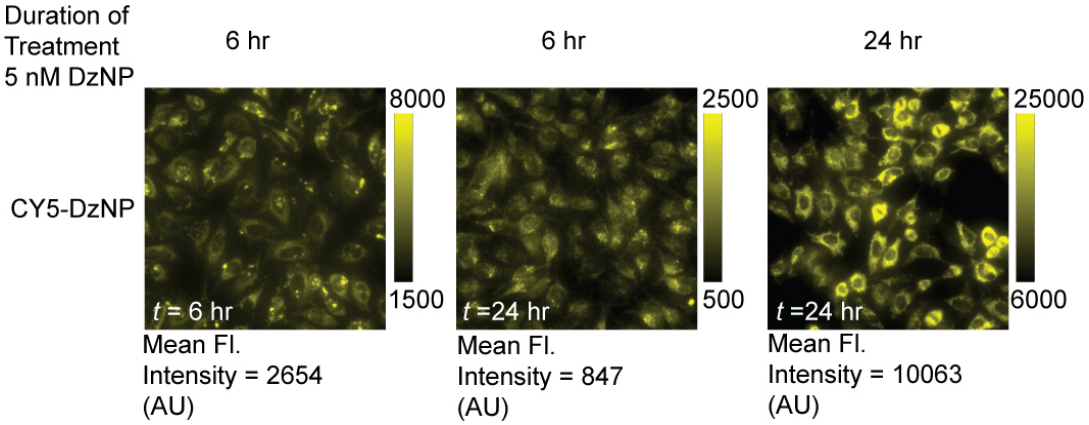

Figure S10. Qualitative observation of DzNP cellular entry. Fluorescent images of HeLa cells treated with 5 nM DzNPs that were hybridized to a complementary oligonucleotide conjugated to a Cy5 fluorescent probe. Fluorescence images were collected at 6 and 24 hour time points. One sample was treated with DzNPs for 6 hrs while the second sample was treated for a 24 hr duration. The fluorescence image at the earlier time point (*t* = 6 hr) shows punctuate signal within the cytoplasm of cells. Cells that were imaged at the 24 hr time point show more uniform and less punctate fluorescence intensity within the cytoplasm. In addition, the cells continually take up DzNPs and cells that were treated for 24 hrs show one order of magnitude larger fluorescence intensity when compared to cells that were only treated with DzNPs for 6 hrs.